PHYSICAL REVIEW B VOLUME 3, NUMBER 10 15 MAY 1971

Critical Concentration for Single-Ion–Single-Ion Energy Transfer in Ruby†

S. K. Lyo
Physics Department, University of California, Los Angeles, California 90024
(Received 8 September 1970)

The critical concentration for single-ion–single-ion energy transfer in ruby is calculated using Anderson's method for transport between ions which are characterized by inhomogeneously broadened energy levels. The excitation on the chromium impurity is assumed to propagate by virtue of superexchange interactions. Using a continuum approximation, we find that the single-ion excitation is localized below concentrations of ~ 0.3–0.4%, a range not inconsistent with that concentration at which a sudden change in the fluorescent lifetime of ruby occurs.

I. INTRODUCTION

It is known that single-ion–single-ion energy transfer in ruby allows for the destruction of laser efficiency as the chromium-ion concentration is increased. Imbusch[1] has shown experimentally that this is caused by R-line excitations propagating from single-ion site to single-ion site until they find an ion-pair "sink" which drains the optical energy nonradiatively to the lattice. The number of chromium pairs increases as the square of the Cr^{3+} concentration, while the number of single ions increases linearly with the Cr^{3+} concentration. Therefore the ratio of the intensities of the pair lines N_1(7041 Å) and N_2(7009 Å) to the R line is expected to increase linearly with Cr^{3+} concentration. However, Schawlow *et al.*[2] observed that the ratio increases faster than linear and concluded that pairs draw energy from the single ions. As the Cr^{3+} concentration is further increased, the N lines become even more intense, the N-line intensities becoming comparable to the R lines at 1% Cr^{3+} concentration. Imbusch observed that N lines exhibit a double decay time at a Cr^{3+} concentration of 0.2%; at this concentration the N lines initially decay rapidly with a decay rate identical to that exhibited by the N lines at the much smaller concentration of 0.044%. During the later part of the decay period, however, the N lines exhibit the much slower decay rate appropriate to the isolated R_1 line. From these data Imbusch concluded that energy must be continually transferred from the single-ion "bath," by means of a single-ion–single-ion energy-transfer mechanism, to the pairs. His argument proceeds as follows: First, the single-ion–pair energy transfer is nonradiative. Therefore, only single ions close to pairs can transfer excitation directly to the pairs. These single ions will decay faster than the main body of single ions. If no spatial transfer occurs (or occurs very slowly) within the single-ion energy reservoir, this fast decay rate should be exhibited in the later part of the N-line decay curve, the intrinsic decay rate of the pair lines being much faster than the decay rate of the neighboring single ions to pairs. Because Imbusch observed that, in fact, the decay rate in the tail of the N-line decay curve is the *same* as for that of the isolated R line, a sufficiently rapid single-ion–single-ion energy-transfer rate must be present.

As the Cr^{3+} concentration is lowered, evidence of single-ion–single-ion energy transfer disappears. The later part of the decay rate of the N lines is as fast as the initial part—no slowly decaying tail is evident for $C < 0.2\%$. In this paper, we contend that this behavior can be understood in terms of a sudden disappearance of single-ion–single-ion energy transfer, necessary to "feed" the N lines, at concentrations below 0.4% (the apparent discrepancy with the above data will be explained later in this section). This sudden disappearance of energy transport as a function of decreasing concentration is a result of the inhomogeneous broadening of R lines due to the strain field, and the large mean distance between the single ions, which we claim localize the R-line excitation and inhibit single-ion–single-ion transfer. According to a calculation of Anderson,[3] below a critical concentration of Cr^{3+} ions, this localization is complete—no single-ion–single-ion transfer can occur. It is essential in such a model that the strain be microscopic compared to the (approximately) six atom spacing corresponding to the nearest-neighbor chromium distance at the critical concentration of 0.4%, causing random distribution of energy levels for all chromium sites.

Stated again for clarity, we claim Anderson's[3] most probable path diffusion model for inhomogeneously broadened systems results in a critical concentration below which single-ion–single-ion energy transport cannot occur. The scarcity of pair sites requires this transport for any significant degradation of the single-ion fluorescent lifetime. Experimentally, it appears that the intrin-

sic fluorescent lifetime for the R line in ruby drops abruptly above a critical concentration (~ 0.4 at.%) of chromium ions. We argue that, for concentrations below this value, localization of the single-ion excitation (in the sense of Anderson[3]) obtains, and R-line energy flow to the pair sites is inhibited. For concentrations above this value, we argue that the single-ion excitations are delocalized, energy flow occurs within the single-ion system, and the pair sites are able to drain off significant R-line intensity as manifested in the sharply larger value of the fluorescent decay rate and the sharp rise in the N-line intensities.

The possibility of localization of an excitation propagating in an inhomogeneously broadened system was first studied by Anderson.[3] He investigated in specific terms the motion of an electron in an impurity band making quantum jumps from a donor (acceptor) site to another donor (acceptor) site whose energy levels (ground states) are randomly distributed because of Coulomb interactions with randomly placed charged centers. He argued that the electron will be localized (and no longer mobile) at a particular site, should the inhomogeneous width exceed by several times the site transfer interaction strength (the exact requirement depending upon the crystal structure and the number of nearest neighbors).

The efficiency of the single-ion–single-ion interaction depends on two factors: (i) the concentration which determines the mean distance between impurity centers and (ii) the width of the inhomogeneous broadening which "detunes" the resonance frequency of the interacting sites. According to a model of Anderson,[3] localization of the excitation on a single ion is expected for concentrations below a critical value, increasing for increasing inhomogeneous broadening.

To calculate the critical concentration, we use Anderson's most probable path method.[3] He chose the self-energy part [$V_c(s)$, see Sec. II, Eq. (6)] of the Green's function as a suitable quantity to be studied and argued that if the most probable value of the imaginary part becomes zero as $\mathrm{Re}(s) \to +0$, then localization obtains. Lloyd,[4] however, has shown that by taking the average value of the full Green's function, no localization is possible for any type of interaction. This difference of opinion arises in the following way: The probability distribution of $\mathrm{Im}V_c(s)$ as $\mathrm{Re}(s) \to +0$, is not sharply peaked at its average value, unlike other quantities such as the density of states. This is because an infinitesimal fraction of sites contribute an infinite amount to $\lim[\mathrm{Im}V_c(s)]$ as $\mathrm{Re}(s) \to +0$. This can be seen even from the first term of the series for $V_c(s)$ [Eq. (6)]. For transfer interactions falling off faster than $1/r^3$, $\lim[\mathrm{Im}V_c(s)]$ as $\mathrm{Re}(s) \to +0$ will have zero value with almost unit probability for most of the configurations of the random impurity energy levels. This means that we will almost always have localization (keeping only the first term of the series for the sake of argument). However, due to an infinitesimal fraction of sites which possess energies which cause the denominators to vanish, the average will be nonzero, leading to a conclusion that transport obtains. This is due to the fact that the averaging process smears out the discrete poles on the imaginary axis into a branch cut which will cause a finite discontinuity of the self-energy term at the imaginary axis. This results in a nonvanishing value for $\lim[\mathrm{Im}V_c(s)]$ as $\mathrm{Re}(s) \to +0$, leading to a delocalization. This is, however, an erroneous conclusion resulting from the *incorrect* assumption that the average is a *representative* value.[3,5] Put another way, because we are interested only in how often the experiment tells us $\lim[\mathrm{Im}V_c(s)]$ as $\mathrm{Re}(s) \to +0$ is zero (localization) and nonzero (delocalization), it is meaningless to take the average; the weighted average of zero and nonzero elements is always nonzero, obscuring the fact that for the overwhelming majority of configurations $\lim[\mathrm{Im}V_c(s)]$ as $\mathrm{Re}(s) \to +0$ is zero when localization is dominant.

Our result exhibits localization of the R-line excitation below a chromium concentration of ~ 0.3–0.4%. We believe that this can explain the concentration dependence of the R-line decay time in thin ruby samples as shown in Fig. 1.[1,6] It is seen there that the flourescent lifetime decreases abruptly for concentrations greater than approximately 0.4%. However, Imbusch's data of N-line double decay at 0.2% of Cr^{3+} concentration imply that some single-ion–single-ion energy transfer is present even at this concentration, although the weak N-line intensity shows that the rate is very small. The presence of this weak residual single-ion–single-ion interaction below the critical concentration may possibly be due to other types of interactions (e.g., long-range magnetic dipolar interactions). However weak these may be, they always result in energy transport, according to Anderson's theory. We contend that the dominant energy-transfer mechanism is the exchange interaction, which being short range in character, will exhibit sharp localization at low concentrations. The absence of R_1-line single-ion–single-ion energy transfer at the low concentration of 0.05% was recently observed by Szabo.[7]

II. SUMMARY OF ANDERSON'S METHOD

The following is a brief summary of Anderson's theory.[3] The basic Schrödinger equation is

$$i\dot{A}_{\vec{i}}(t) = E_{\vec{i}}A_{\vec{i}}(t) + \sum_{\vec{i}\neq\vec{j}} V_{\vec{j}\vec{i}}A_{\vec{i}}(t)\,, \tag{1}$$

where $\hbar = 1$, $A_{\vec{j}}(t)$ is the probability amplitude at

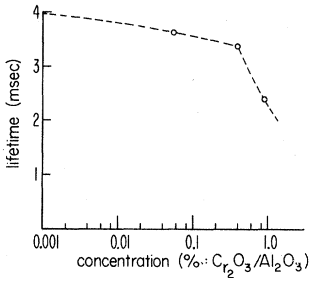

FIG. 1. Plot of R-line decay time measured at 77 °K as a function of chromium concentration on very small samples of ruby (Refs. 1 and 6).

site $\vec{j}$ at time t, $E_{\vec{j}}$ is the random energy at the impurity given by a probability function $P(E_{\vec{j}})$, and $V_{\vec{j}\vec{l}}$ is a small perturbation representing the interaction strength between sites $\vec{j}$ and $\vec{l}$. In our problem $E_{\vec{j}}$ is the energy spacing between $^4A_2$ and ^2E levels at site $\vec{j}$, which is inhomogeneously broadened by strain field. Also $V_{\vec{j}\vec{l}}$ is the exchange interaction between the two sites [see Eq. (22)]. Assuming that the excitation starts from site $\vec{l}$ initially ($t=0$), i.e.,

$$A_{\vec{j}}(0)=\delta_{\vec{l}\vec{j}}\,, \tag{2}$$

where $\delta_{\vec{l}\vec{j}}$ is the Kronecker δ, we can calculate $A_{\vec{l}}(\infty)$. If $A_{\vec{l}}(\infty)\neq 0$, the excitation will remain at the original site with finite probability an infinite time later. This is the basic definition of the Anderson's localization. In order to put this condition in terms of more convenient variables, we start by taking the Laplace transform of (1). Using the initial condition (2), one obtains

$$f_{\vec{j}}(s)=\frac{i\delta_{\vec{l}\vec{j}}}{is-E_{\vec{j}}}+\sum_{\vec{k}\neq\vec{j}}\frac{1}{is-E_{\vec{j}}}\,V_{\vec{j}\vec{k}}f_{\vec{k}}(s)\,, \tag{3}$$

where

$$\begin{aligned} f_{\vec{j}}(s)&=\int_0^\infty e^{-st}A_{\vec{j}}(t)dt\,,\\ A_{\vec{j}}(t)&=\frac{1}{2\pi i}\int_{-i\infty+\gamma}^{i\infty+\gamma}f_{\vec{j}}(s)\,e^{st}\,ds\,, \end{aligned} \tag{4}$$

γ is an arbitrary positive real value such that $f_{\vec{j}}(s)$ is analytic for $\mathrm{Re}(s)>\gamma$. By iteration it follows that

$$f_{\vec{l}}(s)=i/[is-E_{\vec{l}}-V_c(s)]\,, \tag{5}$$

with

$$V_c(s)=\sum_k{}'\,V_{\vec{l}\vec{k}}\times\left(\frac{V_{\vec{k}\vec{l}}}{is-E_{\vec{k}}}+\sum_{\vec{i}}\frac{V_{\vec{k}\vec{i}}V_{\vec{i}\vec{l}}}{(is-E_{\vec{k}})(is-E_{\vec{i}})}+\cdots\right)\,, \tag{6}$$

where $\sum'$ means summing on nondiagonal indices.

The Green's function $f_{\vec{l}}(s)$ is analytic on the right half of the S plane and in general has a cut on the imaginary axis. Therefore we can put $\gamma\to+0$ in (4) and push the contour across the imaginary axis to negative infinity, taking all the contributions from the poles on the left half of the plane. For $t\to+\infty$, the dominant contribution comes from a pole closest to the imaginary axis. Thus the amplitude $A_{\vec{l}}(t)$ will decay at a rate of $e^{-t/\tau}$ with τ given by

$$1/\tau=\lim[\mathrm{Im}V_c(s)]\ \text{ as }\ \mathrm{Re}(s)\to+0. \tag{7}$$

When $\lim[\mathrm{Im}V_c(s)]=0$, as $\mathrm{Re}(s)\to+0$ the discontinuity at the imaginary axis disappears, and the cut is reduced to poles located on the imaginary axis. Therefore $A_{\vec{l}}(t)$ becomes oscillatory with time, resulting in a localization. The imaginary part of s is determined by setting the real part of the denominator of (5) to zero:

$$-\mathrm{Im}s=E_{\mathrm{I}}+\mathrm{Re}V_c(s)\,.$$

This equation, combined with (6), is just the Brillouin-Wigner perturbation series, which contains all the eigenstates of the system. Hence (5) has poles in the vicinity of each $E_{\vec{k}}'s$. However, the residues become extremely small as we depart from $E_{\vec{l}}$. Therefore we are to consider a pole only in the neighborhood of $E_{\vec{l}}$. We take s real (in the following we will take s as positive infinitesimal), and replace $E_{\vec{k}}$ by $E_{\vec{k}}'=E_{\vec{k}}-E_{\vec{l}}-\mathrm{Re}V_c(s)$. In practice we shall ignore the energy shift $\mathrm{Re}V_c(s)$, so that

$$E_{\vec{k}}'=E_{\vec{k}}-E_{\vec{l}}\,. \tag{8}$$

For convenience, following Anderson, we shall take the energy $E_{\vec{l}}$ to lie at the center of the original band (or origin of the energy scale) so that $E_{\vec{k}}'=E_{\vec{k}}$. The basic difficulty of the problem arises from the fact that $V_c(s)$ is a function of stochastic variables, $E_{\vec{k}}$, $E_{\vec{l}}$, ... Therefore we can treat $V_c(s)$ only in the sense of probability. It is at this point that Anderson's approach differs basically from that of Lloyd, as discussed in the Introduction. If $\lim V_c(s)$ as $s\to+0$ converges (in the most probable sense), then $1/\tau=\lim[\mathrm{Im}V_c(s)]=0$ as $s\to+0$, and we have localization. Anderson showed that the first term of (6) diverges for an interaction $V_{\vec{j}\vec{l}}$ falling off as $1/r_{\vec{j}\vec{l}}^3$ or slower with distance, leading to transport. Thus, dipolar interactions always give delocalization. If the interaction falls off faster than $1/r^3$, then the first term converges. (In our case, superexchange interactions are used for $V_{\vec{j}\vec{l}}$. They typically exhibit exponential range dependences.) However, as memtioned earlier, the average of the imaginary part of the first term, essentially the Golden rule result, is nonzero. This should not be interpreted as an indication of delocalization, since the average

is meaningless for the reason explained in the Introduction. Therefore we must go to higher-order terms to see if transport occurs.

Define a random variable T_L as

$$T_L = \left| \frac{V_{k_1 k_2} \cdots V_{k_L I}}{(is - E_{k_1}) \cdots (is - E_{k_L})} \right|_{(s \to +0)} . \quad (9)$$

This is an absolute value of a term appearing in the $(L-1)$ th summation in the bracket of (6). Then the average number of terms with a magnitude between T_L and $T_L + dt_L$ in the $(L-1)$ th summation in the large parentheses of (6) can be shown to be, for a large L [see Eq. (34)],

$$n(T_L)\, dT_L = \left[F\left(\frac{W}{V}\right) \right]^L \frac{d\,T_L}{T_L^2}\, L(T_L) \quad (L \gg 1) , \quad (10)$$

where F is a certain function to be calculated, $L(T_L)$ is a slowly varying function of T_L, W is the width of the inhomogeneous broadening [see Eq. (20)], and V is a parameter representing the interaction strength. The probability distribution of

$$\Sigma_L = \sum_{(k_1 k_2 \cdots k_L)} (\pm T_L)$$

is given by

$$P(\Sigma_L)\, d\Sigma_L \sim \left[F\left(\frac{W}{V}\right) \right]^L \frac{d\,\Sigma_L}{\Sigma_L}\, L(1) \quad (L \gg 1) . \quad (11)$$

If one defines $(W/V)_0$ to satisfy

$$[F((W/V)_0)]^L\, L(1) = 1 , \quad (12)$$

then, as $L \to \infty$, the series (V_c) will converge with a probability $\sim 1 - e^{-L}$, if

$$W/V > (W/V)_0 . \quad (13)$$

Equation (13) is Anderson's criterion for localization. To find the function F, define

$$T = \left(\frac{V_{\max}}{\frac{1}{2} W} \right)^L e^{\Xi + \Sigma} , \quad (14a)$$

$$e^{\Sigma} = \prod_{j=1}^{L} \left(\frac{V_j}{V_{\max}} \right) , \quad (14b)$$

$$e^{\Xi} = \prod_{j=1}^{L} \left| \frac{\frac{1}{2} W}{is - E_j} \right| \quad (s \to +0) , \quad (14c)$$

$$T = \left(\frac{V_{\max}}{\frac{1}{2} W} \right)^L e^{X} , \quad (14d)$$

V_j representing an arbitrary factor $V_{kk'}$ in the numerator of (9). It is convenient to take the bilateral Laplace transform of the distribution function $P(\Sigma)$ of the variable Σ:

$$\Phi(p) = \int_{-\infty}^{\infty} P(\Sigma)\, e^{-p\Sigma}\, d\Sigma . \quad (15)$$

Similarly we can take the bilateral Laplace transform probability distribution function $P(\Xi)$ of the variable Ξ:

$$\Psi(p) \int_{-\infty}^{\infty} P(\Xi)\, e^{-p\Xi}\, d\Xi . \quad (16)$$

In practice, the evaluation of (15) and (16) encounters a difficulty arising from the correlation of the factors in (9). To eliminate this correlation, Anderson used a multiple-scattering formalism. The repeated scattering from the same site corresponding to the repetition of the same indices in (6) can be removed by modifying the site energies in a self-consistent way. Because the path will not involve visits to the same site twice, the correlation is removed. However, we have to make proper account for the modified energy denominators. Anderson argued that the consequence of the prohibition of repeated indices is to reduce the large terms in the series, so that the series will be more easily convergent, unless $|e_k| \geq V^2/W$, where e_k is the modified energy denominator. He used this condition as a restriction on the modified energy terms. This limitation arises at the expense of removing the correlation. He argued that this limitation is not of importance, and that removing this restriction will give the upper limit of the critical value of $(W/V)_c$. Thus, actual localization is more easily achieved than will be exhibited neglecting these correlations, and we will underestimate the critical concentration. The error is small if the condition $W \gg V$ is satisfied. This condition is well satisfied in our problem as will be shown later, and we shall adopt this approximation. By defining $\Lambda(p)$ as the bilateral Laplace transform of the total distribution function $n(X)$

$$\Lambda(p) = \int_{-\infty}^{\infty} n(X)\, e^{-pX}\, dX , \quad (17)$$

one obtains by convolution that

$$\Lambda(p) = \Phi(p)\, \Psi(p) . \quad (18)$$

The relation $X = \Sigma + \Xi$ obtained from (14a) and (14d) is used. Thus $n(X)$ can be obtained through the inverse Laplace transformation,

$$n(X) = \frac{1}{2\pi i} \int_{-i\infty + \gamma}^{i\infty + \gamma} \Lambda(p)\, e^{pX}\, dp , \quad (19)$$

where γ is the real part of p in (15) and (16). γ is generally restricted to a region where (15) and (16) are well defined and do not diverge. Using (14), (19) can be put into the form of (10).

III. EVALUATION OF CRITICAL CONCENTRATION

This section deals with the diffusional motion of a single-ion excitation ($^4A_2 \to {}^2E$) in ruby using the scheme developed in Sec. II.

The energy levels of the impurity chromium ions are inhomogeneously broadened due to the strain

field. We assume that this broadening is described by a rectangular probability distribution centered at the origin:

$$P(E_{\vec{j}}) = 1/W, \quad -\tfrac{1}{2}W \le E_{\vec{j}} \le \tfrac{1}{2}W$$
$$= 0, \qquad |E_{\vec{j}}| > \tfrac{1}{2}W \ . \tag{20}$$

A modification of this distribution function will affect our results. For example, if we enhance the central part of the distribution with respect to the wings, the energy levels are less disturbed by the random "potential." The critical concentration will be lowered, because the excitation will be more easily delocalized. We have not carried out any numerical estimate for such a modification. Our point in this paper is merely to present a theoretical basis for the observations of Imbusch. Other approximations we are forced to make will also detract from quantitative conclusions. For all these reasons, we must stress that the numerical results of this paper should not be taken too seriously. However, the fact that our final value for the critical localization concentration is in the vicinity of that derived from Imbusch's experiments does demonstrate that something like the model we are using applies to dilute ruby. Further theoretical refinements await a more complete experimental study of the concentration dependence of fluorescent decay curves for the R and N lines.

As an example of the kind of approximation we have been forced to make, the inhomogeneous broadening has been assumed microscopic in character. Should the reverse be true, there may be some suspicion that even in the dilute regime resonant sites obtain for ions at the average ion-ion separation. At a Cr^{3+} concentration of 0.4%, the average distance between nearest chromium neighbors will be about six atomic spacing. Should broadening be more macroscopic than these distances, nearby chromium sites will be resonant and our estimate of the critical concentration will be too large. Indeed, in the limit of large macroscopic correlation lengths for the broadening interaction, localization will not occur. We contend that the experiments of Imbusch mitigate this conclusion. Using (14c) and neglecting correlation, we evaluate (16):

$$\Psi(p) = \int_{-\infty}^{\infty} P(\Xi) e^{-p\Xi}\, d\Xi = \langle e^{-p\Xi} \rangle$$
$$= \left(\int_{-W/2}^{W/2} \left| \tfrac{1}{2}W/E \right|^{-p} P(E)\, dE \right)^{L}$$
$$= 1/(1+p)^{L} \quad (-1 < p, \quad L \gg 1). \tag{21}$$

The mechanism for energy transfer in dilute ruby first proposed by Imbusch was the electric quadrupole-quadrupole interaction. He argued that exchange (incorrectly), magnetic dipole-dipole, and electric dipole-dipole mechanisms were several orders of magnitude too weak to account for the rapid single-ion–single-ion energy-transfer rate. However, Birgeneau[8] contended that errors entered in Imbusch's estimates of the relevant matrix elements and interaction strengths. He demonstrated that the electric quadrupolar oscillator strength was overestimated by Imbusch (the mixing matrix elements were taken too large) and that off-diagonal (in total spin) exchange interactions can indeed contribute to the single-ion–single-ion energy-transfer rate. A reasonable value of the single-ion–single-ion exchange integral $J = 2.5 \times 10^{-3}$ cm^{-1} for ions separated by an average of 13 Å led to microsecond transfer rates as required experimentally. Later, Huang[9] showed from detailed calculations that the magnitude of the energy-transfer integral for single-ion–single-ion energy transfer between V^{2+} ions in $KMgF_3$ host separated by three F^- ions is indeed about 10^{-3} cm^{-1}, indirectly supporting Birgeneau's theory. The short-range interaction model of Birgeneau was further supported recently by Szabo.[10]

Therefore, in this paper, we shall adopt Bigeneau's model for single-ion–single-ion interactions. We assume the chromium impurities are coupled by superexchange interactions, the range dependence of which can be approximated by

$$V_{\vec{j}\vec{l}} = V_0 S^{N(\vec{r}_{\vec{j}\vec{l}})}, \tag{22}$$

where S is an overlap integral, $N(\vec{r}_{\vec{j}\vec{l}})$ is the number of oxygen bonds between sites $\vec{j}$ and $\vec{l}$, and V_0 is a positive constant. We can estimate $N(\vec{r}_{\vec{j}\vec{l}})$ by

$$N(\vec{r}_{\vec{j}\vec{l}}) = 2\mu(\theta, \phi) r_{jl}/a, \tag{23}$$

where $r_{jl} = |\vec{r}_{\vec{j}} - \vec{r}_{\vec{l}}|$ and a is a fourth-neighbor distance for Al ions in Al_2O_3. μ varies between $\mu = 1$ and μ 1.7. In Fig. 2 we show the approximate angular dependence of μ (solid line) on one of the reflection symmetry planes (σ_d) of the group D_{3d} appropriate to ruby. Using (23), we can rewrite (22):

$$V(\vec{r}) = V_0 \exp\{-[\mu(\theta, \phi)/a_0] r\}, \tag{24}$$

where $a_0^{-1} = 2a^{-1} \ln S^{-1}$. Using the above equation and (14b), we can calculate (15), again ignoring correlation and using the continuum approximation,

$$\Phi(p) = \int_{-\infty}^{\infty} p(\Sigma) e^{-p\Sigma}\, d\Sigma = \langle e^{-p\Sigma} \rangle$$
$$= \left[\int_{r_0}^{\infty} \left(\frac{V_0}{V_{\max}} \right)^{-p} \exp \frac{p\mu(\theta, \phi) r}{a_0}\, n_0\, d^3\vec{r} \right]^{L}$$
$$(p < 0, \quad L \gg 1), \tag{25}$$

where n_0 is the density of impurities and r_0 is the

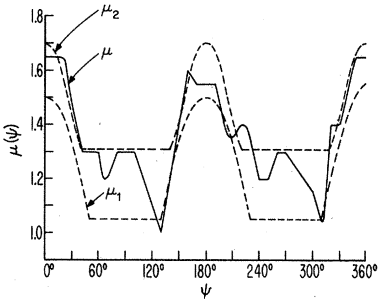

FIG. 2. Plot of μ defined in Eq. (23) versus the plane polar angle (Ψ) measured from the c axis on one of the σ_d planes. μ_1 [Eq. (26)] and μ_2 [Eq. (45)] are the approximate lower and upper limits, respectively.

ensemble average of the minimum distance of approach between the impurities. The concentration dependence of the criterion (12) is introduced via this parameter. Although it is possible to evaluate (25) quite accurately numerically, it is not particularly useful because it is almost impossible to carry out the inverse Laplace transform (19) using the complicated dependence of $\Phi(p)$ on p. Therefore, we only attempt to set upper and lower limits of the critical concentration by bounding $\mu(\theta,\phi)$ above and below with curves μ_1 and μ_2 defined in Fig. 2. The process is continued until we obtain a satisfactorily small enough difference. μ_1 (μ_2) will overestimate (underestimate) $V(\vec{r})$ and give the lower (upper) limit of the critical concentration.

The quantities μ_1 and μ_2 are also chosen in such a way that we are able to use the following approximations: (a) axial symmetry around the c axis and (b) the reflection symmetry about the plane of $\theta=\frac{1}{2}\pi$ in the low-concentration limit.

A. Lower Limit of Critical Concentration

Given

$$\mu_1(\theta,\phi)=0.25+1.25|\cos\theta|,$$
$$0\le\theta\le 50^\circ,\quad 130^\circ\le\theta\le 180^\circ$$
$$=1.05,\qquad 50^\circ\le\theta\le 130^\circ \tag{26}$$

(25) can be evaluated to yield

$$\Phi(p)=\left\{4\pi n_0\left(\frac{V_0}{V_{\max}}\right)^{-p}\int_{r_0}^{\infty}dr\,r^2 \times\left[\int_0^{50^\circ}d\theta\sin\theta\exp\left(\frac{0.25+1.25\cos\theta}{a_0}pr\right)+\int_{50^\circ}^{90^\circ}d\theta\sin\theta\exp\left(\frac{1.05}{a_0}pr\right)\right]\right\}^L \quad (p<0). \tag{27}$$

It is convenient to define a parameter η by

$$\eta=r_0/a_0. \tag{28}$$

Since $V_{\max}=V_0\exp[-(1.05/a_0)r_0]$, one finds

$$(V_0/V_{\max})=e^{1.05\eta}. \tag{29}$$

We continue our integration by substituting (28) and (29) into (27):

$$\Phi(p)=\left\{4\pi n_0a_0^3e^{-1.05p\eta}\left[-\frac{1}{1.25p}\left(\frac{1}{(1.05p)^2}-\frac{\eta}{1.05p}\right)e^{1.05p\eta}+\frac{1}{1.25p}\left(\frac{1}{(1.50p)^2}-\frac{\eta}{1.50p}\right)e^{1.50p\eta}+\cos50^\circ\left(-\frac{2}{(1.05p)^2}+\frac{2\eta}{(1.05p)^2}-\frac{\eta^2}{1.05p}\right)e^{1.05p\eta}\right]\right\}^L \quad (p<0). \tag{30}$$

We can now compute (19), using (21) and (30). The path of the integral is restricted to a strip with $-1<\gamma<0$ (Fig. 3). Since we are interested in X with a positive real part, we deform the contour to negative infinity as shown by C_1. We can further modify this contour to an arbitrarily small circle (C_2) around $p=-1$ by noticing that this is the only pole in the left half of the plane. Thus, only the infinitesimal neighborhood at $p=-1$ will be important. Therefore, anticipating that $\eta\gg1$, we can neglect the second term in the bracket of (30), which allows us to rewrite the remaining terms as

$$\Phi(p)=\left\{\frac{0.643}{1.05}4\pi n_0a_0^3\frac{1}{-p}\left[\left(\eta-\frac{1.57}{p}\right)^2+\frac{0.6}{p^2}\right]\right\}^L.$$

Neglecting the second term in the bracket, one obtains

$$\Phi(p)=\left[\frac{0.643}{1.05}4\pi n_0a_0^3\frac{1}{-p}\left(\eta-\frac{1.57}{p}\right)^2\right]^L \quad (p<0), \tag{31}$$

which, combined with (21), gives

$$n(X)=\frac{1}{2\pi i}\left(\frac{0.643}{1.05}\,4\pi n_0 a_0^3\right)^L\int_{C_2} dp\,\frac{1}{(1+p)^L}\,\frac{1}{(-p)^L}\left(\eta-\frac{1.57}{p}\right)^{2L}e^{pX}. \tag{32}$$

This can be evaluated for $L\gg 1$ as (see Appendix A)

$$n(X)\sim\left(\frac{0.643}{1.05}\,4\pi n_0 a_0^3 e^{0.959\pm 0.0537}\right)^L e^{-X}\left(\eta+1.57e^{0.00289}\right)^{2L}$$

$$\times\left(\frac{X}{L}+1.50+\frac{2}{1+\eta/1.57e^{0.00289}}\right)^L \qquad (L\gg 1) \tag{33}$$

or, in terms of T, using (14d) and (28),

$$n(T)dT\sim\left(\frac{0.643}{1.05}\,4\pi n_0 r_0^3\eta^{-3}e^{0.959\pm 0.0537}\right)^L\left(\frac{2V_{\max}}{W}\right)^L\left(\eta+1.57e^{0.00289}\right)^{2L}$$

$$\times\left(\frac{\ln T}{L}+\ln\frac{W}{2V_{\max}}+1.50+\frac{2}{1+\eta/1.57e^{0.00289}}\right)^L\frac{dT}{T^2}. \tag{34}$$

The criterion for localization (12) is now

$$6.39\pi e^{\pm 0.0537}f\eta^{-3}\left(\frac{2V_{\max}}{W}\right)(\eta+1.62)^2\left(\ln\frac{W}{2V_{\max}}+1.50+\frac{2}{1+\eta/1.62}\right)=1, \tag{35}$$

with f defined as

$$f=n_0 r_0^3. \tag{36}$$

Assuming a random distribution of the impurities, f is found to be (Appendix B)

$$f=\frac{3}{4\pi}\,\Gamma\left(\tfrac{4}{3}\right)^3\simeq 0.170 \quad (\Gamma=\gamma\text{ function}). \tag{37}$$

A typical exchange integral J, appropriate to geometries and distances where cation-cation effects can certainly be neglected, is given by the interaction strength between fourth chromium neighbors in the perfect Cr_2O_3 lattice. Because these are linked by two oxygen bonds, it follows from our model that

$$J=V_0S^2 \tag{38}$$

which, combined with (29), gives

$$\eta=\frac{1}{1.05}\left(\ln\frac{W}{2V_{\max}}+\ln\frac{2J}{W}+2\ln S^{-1}\right). \tag{39}$$

The critical value of the ratio $W/2V_{\max}$ is obtained from (35) and (39). If $\tilde{n}$ is the density of Al in the perfect Al_2O_3 and C is the impurity concentration, then n_0 is given by

$$n_0=\tilde{n}C. \tag{40}$$

$\tilde{n}$ is found directly from the crystal structure and is given by

$$\tilde{n}=2.00/a^3. \tag{41}$$

Then Eqs. (28) and (36)–(41) give

$$C=0.085(2\ln S^{-1}/\eta)^3. \tag{42}$$

Substitution of representative values for the exchange J, for the inhomogeneous width W of the R line, and for the overlap integral S,

$$J=10\text{cm}^{-1}\text{ (Ref. 11)},\quad W=0.14\text{cm}^{-1}\text{ (Ref. 12)},\quad S=0.3\text{ (Ref. 13)} \tag{43}$$

yields

$$(W/2V_{\max})\sim 1.4\text{–}1.7$$

or a lower limit to the critical concentration

$$(C_{\text{crit}})_{\text{lower}}=0.3\%, \tag{44}$$

a result corresponding to the lower curve μ_1 in Fig. 2. Although the ratio $W/2V_{\max}$ is not much larger than unity, our approximation of neglecting correlation in (21) and (25) is valid because the number of the neighbors is very small and $V(r)$ is a very rapidly decreasing function of the distance. It can also be shown that the excitation is delocal-

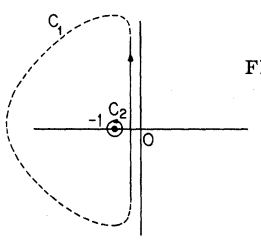

FIG. 3. Contours on the p plane.

ized above this concentration (Appendix C).

B. Upper Limit of Critical Concentration

In this case μ_2 is given by (Fig. 2)

$$\mu_2(\theta,\phi) = -0.44 + 2.14|\cos\theta|, \quad 0 \le \theta \le 40^\circ,\ 140^\circ \le \theta \le 180^\circ$$

$$= 1.21, \quad 40^\circ \le \theta \le 140^\circ. \tag{45}$$

The criterion for localization is found in a similar way:

$$6.60\pi e^{\pm 0.0537} f \eta^{-3} \left(\frac{2V_{\max}}{W}\right)(\eta + 1.16)^2 \times \left(\ln\frac{W}{2V_{\max}} + 1.50 + \frac{2}{1+\eta/1.16}\right) = 1, \tag{46}$$

with

$$\eta = \frac{1}{1.21}\left(\ln\frac{W}{2V_{\max}} + \ln\frac{2J}{W} + 2\ln S^{-1}\right). \tag{47}$$

The critical concentration is again given by (42). Using the parameters (43), we find

$$W/2V_{\max} \sim 1.6\text{–}1.9$$

or, an upper limit to the critical concentration

$$(C_{\text{crit}})_{\text{upper}} = 0.4\%. \tag{48}$$

For the other parameters remaining the same, but for differing overlap integrals S, we find values for the lower and upper limits of the critical concentration which are displayed in Fig. 4. As mentioned earlier, the critical concentration is calculated for the energy at the center of the original band. For an arbitrary energy, one must use the energy differences E_k' instead of E_k. Since the width W' of the probability distribution of E_k' is approximately twice as large as W, we can replace W by $W' = 2W$ in all of the previous equations, obtaining

$$(C_{\text{crit}})_{\text{lower}} \simeq 0.3\text{–}0.4\%, \quad (C_{\text{crit}})_{\text{upper}} \simeq 0.4\text{–}0.5\%.$$

These values are a little larger than those of (44) and (48), respectively (as indeed they should be), meaning that the quantum jump of the excitation is more difficult at energies other than at the center of the original band. Therefore the critical concentration should be determined at the center of the original band.

This method can be applied to other systems such as transition metal and rare-earth crystals by properly accounting for differences of structure and interaction mechanisms. For exchangelike interactions, the structural difference will be manifested through $\mu(\theta,\phi)$ and a_0 in (24). In particular, assuming that the potential decays rapidly beyond the first impurity neighbor, the integral inside the square bracket of (25) will be approximately proportional to the number of the first impurity neighbors at a given concentration. This parameter enters linearly on the left-hand side in the equation which sets the criterion for localization (35). Close examination of the calculation shows that as the number of first impurity neighbors increases, the critical concentration will decrease, indicating that energy transfer is more easily achieved. For the case of ruby we define a nearest neighbor in terms of the number of oxygen ions intervening in the superexchange path. For other, more "orthodox" structures, the number of oxygen links are more closely related to the physical position than in ruby. Thus, a particularly large number of nearest neighbors, at a given concentration, exist in terms of an oxygen linkage definition for ruby, more than, say, for rocksalt type of structures, leading to a lower value for the critical concentration for the former as compared to the latter.

We have neglected the spontaneous emission rate of the R lines compared to the single-ion–single-ion transfer rate. The spontaneous lifetime of R line has an intrinsic value of 4.2 msec. On the other hand, the single-ion–single-ion energy-transfer time is known to be 1–10 μsec at 1% Cr^{3+} concentration. As the Cr^{3+} concentration is lowered, the single-ion–single-ion transfer time increases, becoming infinite at the critical concentration of 0.4% according to our numerical estimates. Because the single-ion–single-ion transfer time is not expected to vary rapidly between a concentration of 1 and 0.4%, we believe that the neglect of the spontaneous emission rate of R lines in com-

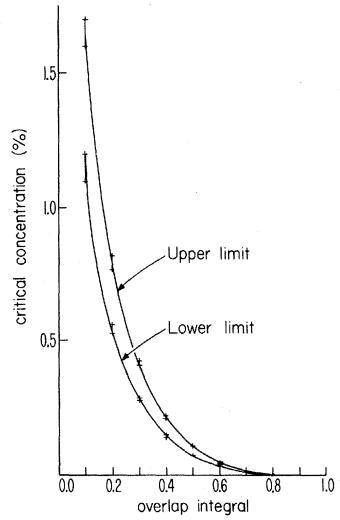

FIG. 4. Critical concentration for single-ion–single-ion energy transfer in ruby.

parison is well justified.

IV. CONCLUSIONS

We have calculated the critical concentration for single-ion–single-ion energy transfer in ruby. We have shown that for concentrations less than ~ 0.3–0.4%, the R-line excitation is localized so that there will be no energy transfer between the single ions, in reasonable agreement with the known data on the fluorescent lifetime of ruby.[1]

ACKNOWLEDGMENTS

I am grateful to Professor R. Orbach for suggesting this problem to me and for many valuable discussions and help in completing the manuscript. Also, I would like to thank R. Chui for his assistance with numerical calculations and E. Yee for valuable help.

APPENDIX A

In this appendix we evaluate the integral

$$I=\frac{1}{2\pi i}\int_{C2} dp\ \frac{1}{(1+p)^L}\ \frac{1}{(-p)^L}\left(A-\frac{B}{p}\right)^{2L} e^{pX}, \tag{A1}$$

where C_2 is a contour shown in Fig. 3 and A, B > 0. Therefore, we obtain

$$I=\text{residue of}\left[\frac{1}{(1+p)^L}\ \frac{1}{(-1)^L}\left(A-\frac{B}{p}\right)^{2L} e^{pX}\right] \quad \text{at } p=-1$$

$$=\frac{1}{(L-1)!}\ \frac{\partial^{L-1}}{\partial p^{L-1}}\left[\frac{1}{(-p)^L}\left(A-\frac{B}{p}\right)^{2L} e^{pX}\right]_{p=-1}$$

$$=\frac{(-1)^L}{(L-1)!}\sum_{\nu=0}^{2L}\binom{2L}{\nu} A^{2L-\nu}(-B)^{\nu}\frac{\partial^{L-1}}{\partial p^{L-1}}\ \frac{e^{pX}}{p^{L+\nu}}\ \Bigg|_{p=-1}$$

$$=\frac{(-1)^L}{(L-1)!}\sum_{\nu=0}^{2L}\binom{2L}{\nu} A^{2L-\nu}(-B)^{\nu} \times\sum_{k=0}^{L-1}\binom{L-1}{k}\frac{\partial^k}{\partial p^k}\ e^{pX}\frac{\partial^{L-1-k}}{\partial p^{L-1-k}}\ \frac{1}{p^{L+\nu}}\ \Bigg|_{p=-1}$$

$$=\sum_{\nu=0}^{\infty}\binom{2L}{\nu}(A)^{2L-\nu}(-B)^{\nu}e^{-X}(Y_\nu)^L, \tag{A2}$$

where we define

$$(Y_\nu)^L=\frac{1}{(L-1)!}\sum_{k=0}^{L-1}\binom{L-1}{k}X^k L^{L-1-k}I(k), \tag{A3}$$

with

$$I(k)=\alpha\left(\alpha+\frac{1}{L}\right)\left(\alpha+\frac{2}{L}\right)\cdots\left(\alpha+\frac{L-2-k}{L}\right)$$

$$\left(\alpha\equiv 1+\frac{\nu}{L}\right).$$

The term $I(k)$ can be put into a closed form, using the fact that $L\gg 1$:

$$\ln I(k)=\sum_{m=0}^{L-2-k}\ln\left(\alpha+\frac{m}{L}\right)=L\int_0^{1-\kappa}\ln(\alpha+t)\,dt$$

$$=L[(-\kappa+\alpha)\ln(1-\kappa+\alpha)+\kappa-1-\alpha\ln\alpha],$$

with

$$\kappa=k/L\ .$$

In order to sum (A3), it is convenient to linearize $\ln I(k)$ in terms of κ:

$$(1/L)\ln I(k)=(1-\kappa)\ln(0.5+\alpha)+\alpha\ln(1+0.5/\alpha) - 0.453\pm 0.0473. \tag{A4}$$

The last term shows the maximum range of error for all values of $0\le\kappa\le 1$. Using (A4), we find

$$(Y_\nu)^L\sim e^L(X/L+0.5+\alpha)^{L-1} \times\exp\{L[\alpha\ln(1+0.5/\alpha)-0.453\pm 0.0473]\}. \tag{A5}$$

It can also be shown that we can linearize the first term in the exponent of the above equation:

$$\alpha\ln(1+0.5/\alpha)=0.0289\,\alpha+0.383\pm 0.0064 =0.0289\,\nu/L+0.412\pm 0.0064\ . \tag{A6}$$

The last term shows the maximum range of the error for all values of ν, i.e., $0\le\nu/L\le 2$.

Therefore, we obtain

$$I\sim e^L e^{-(0.041\pm 0.0537)L}e^{-X}\sum_{\nu=0}^{2L}\binom{2L}{\nu}(A)^{2L-\nu} \times(Be^{0.0289})^{\nu}\left(\frac{X}{L}+1.5+\frac{\nu}{L}\right)^{L-1}. \tag{A7}$$

Since the function

$$\binom{2L}{\nu}A^{2L-\nu}(Be^{0.0289})^{\nu}$$

is sharply peaked at

$$\nu_0=\frac{2L}{1+A/Be^{0.0289}}\ ,$$

whereas $(X/L+1.50+\nu/L)^{L-1}$ is slowly varying, (A7) can be approximated as

$$I \sim e^{(0.959\pm0.0537)L}\, e^{-X}\left(\frac{X}{L}+1.50+\frac{\nu_0}{L}\right)\sum_{\nu=0}^{2L}\binom{2L}{\nu} A^{2L-\nu}\,(B\,e^{0.0289})^{\nu}$$

$$= e^{(0.959\pm0.0537)L}\, e^{-X}\,(A+Be^{0.0289})^{2L}\left(\frac{X}{L}+1.50+\frac{2}{1+A/Be^{0.0289}}\right)^{L-1}. \tag{A8}$$

APPENDIX B

In this appendix we derive the probability function for the nearest-neighbor distance in a system of N randomly distributed ions. If the total volume is V and the density is n_0 then the probability $p(r)$ that no particle will be found within the distance r from a certain ion is given by

$$p(r)=\left(1-\frac{\frac{4}{3}\pi r^3}{V}\right)^N=\left(1-\frac{\frac{4}{3}\pi n_0 r^3}{N}\right)^N=\exp(-\tfrac{4}{3}\pi n_0 r^3) \qquad (N\gg 1).$$

Defining $q(r)dr$ as the probability that some particles will be found in $(r, r+dr)$, one obtains

$$p(r+dr)=p(r)\,[1-q(r)dr],$$

which can be rewritten as

$$p(r)q(r)=\frac{\partial p(r)}{\partial r}.$$

However, $p(r)q(r)dr$ is just the probability $P(r)dr$ of finding the nearest neighbors in $(r, r+dr)$. Therefore, we have

$$P(r)=\frac{\partial p(r)}{\partial r}=4\pi n_0 r^2\exp(-\tfrac{4\pi}{3}n_0 r^3).$$

The average is given by

$$r_0=\int_0^\infty r\,P(r)dr=\left(\frac{3}{4\pi n_0}\right)^{1/3}\int_0^\infty x^{4/3-1}\,e^{-x}\,dx$$

$$=\left(\frac{3}{4\pi n_0}\right)^{1/3}\Gamma(\tfrac{4}{3}).$$

Hence

$$r_0^3 n_0=0.170.$$

APPENDIX C

It is convenient to use the quantity [Eq. (7)]

$$1/\tau=-\lim[\mathrm{Im}\,V_c(s)] \quad \text{as } s\to+0 \tag{C1}$$

instead of T_L [Eq. (9)] to prove the delocalization above the critical concentration. The $(L-1)^{\text{th}}$ term of (C1) can be written, to the first order in s, as

$$(-1)^{L-1}\,s\sum_{k_1\cdots k_{L-1}}{}' V_{Ik_1}V_{k_1k_2}\cdots V_{k_{L-1}I}\left(\frac{1}{E_{k_1}^2E_{k_2}\cdots E_{k_{L-1}}}\right.$$

$$\left.+\cdots+\frac{1}{E_{k_1}\cdots E_{k_{n-1}}E_{k_n}^2E_{k_{n+1}}\cdots E_{k_{L-1}}}+\cdots+\frac{1}{E_{k_1}\cdots E_{k_{L-2}}E_{k_{L-1}}^2}\right)=s\sum_n \pm I_n, \tag{C2}$$

where

$$I_n=\left|\frac{V_{Ik_1}V_{k_1k_2}\cdots V_{k_{L-1}I}}{E_{k_1}\cdots E_{k_{n-1}}E_{k_n}^2E_{k_{n+1}}\cdots E_{k_{L-1}}}\right|, \tag{C3}$$

$$I_n=(2V_{\max}/W)^L\,e^X. \tag{C4}$$

Define

$$(\tfrac{1}{2}W)^L\left|\frac{1}{E_{k_1}\cdots E_{k_{n-1}}E_{k_n}^2E_{k_{n+1}}\cdots E_{k_{L-1}}}\right|=e^S, \tag{C5}$$

then Eq. (16) gives

$$\Psi(p)=\frac{1}{2(1+p)^{L-2}(\frac{1}{2}+p)}, \quad p>-\tfrac{1}{2}. \tag{C6}$$

Therefore

$$n(X)=\frac{1}{2\pi i}\int_{-i\infty+\gamma}^{i\infty+\gamma}\frac{\Phi(p)e^{pX}}{2(1+p)^{L-2}(\frac{1}{2}+p)}\,dp, \quad -\tfrac{1}{2}<\gamma<0$$

where $\Phi(p)$ is given by Eq. (30). Integrating around the simple pole at $p=-\frac{1}{2}$,

$$n(X)=\frac{1}{2\pi i}\int_{C_2}\frac{\Phi(p)e^{pX}}{2(1+p)^{L-2}(p+\frac{1}{2})}+2^{L-3}\,\Phi(-\tfrac{1}{2})\,e^{-X/2}, \tag{C7}$$

where C_2 is given in Fig. 3. For $L\gg 1$ it can easily be seen that the first term gives Eq. (33) and the second term is negligible for the value of $W/2V_{\max}$ within the range of our solution. Therefore $\sum_n \pm I_n$

will diverge in a most probable sense above the critical concentration and $1/\tau$ will be nonzero or tend to zero slower than s, leading to a delocalization. (The series converges below the critical concentration; this means that $1/\tau \to 0$ as $s \to 0$, and we have localization.)

†Supported in part by the IBM Graduate Fellowship, the National Science Foundation, and the U. S. Office of Naval Research, Contract No. N00014-69-0200-4006.

[1]G. F. Imbusch, Phys. Rev. 153, 326 (1967).

[2]A. L. Schawlow, D. L. Wood, and A. M. Clogston, Phys. Rev. Letters 3, 271 (1959).

[3]P. W. Anderson, Phys. Rev. 109, 1492 (1958).

[4]P. Lloyd, J. Phys. C 2, 1717 (1969).

[5]P. W. Anderson, Comments Solid State Phys. 2, 193 (1970).

[6]N. A. Tolstoi and Liu Shun'-Fu, Opt. i Spectroskopiya 13, 403 (1962) [Opt. Spectry. (USSR) 13, 224 (1962)].

[7]A. Szabo, Phys. Rev. Letters 25, 924 (1970).

[8]R. J. Birgeneau, J. Chem. Phys. 50, 4282 (1969).

[9]Nai Li Huang, Phys. Rev. B 1, 945 (1970).

[10]Szabo (Ref. 7) observed absence of spectral diffusion of R_1 line over a period of 10 msec for 0.05% ruby. His estimation of single-ion–single-ion energy-transfer rate for 0.05% ruby based on quadrupole-quadrupole interaction gives 10^5 sec^{-1} at 4.2 °K. Because this fast transfer rate would broaden the line appreciably during 10 msec, he concluded that the interaction cannot be multipolar as proposed by Imbusch. However, Golden rule argument as used by Szabo may not necessarily prove or disprove the possibility of quadrupolar interaction, because it is not proper to use the averaging method below a critical concentration; in case the critical concentration for quadrupole-quadrupole interaction is larger than 0.05% (which is quite possible), quadrupole-quadrupole interaction will not exhibit any energy transfer at this low concentration.

[11]F. Keffer and T. Oguchi, Phys. Rev. 115, 1428 (1959).

[12]S. Geschwind, G. E. Devlin, R. L. Cohen, and S. R. Chinn, Phys. Rev. 137, A1087 (1965).

[13]Nai Li Huang, R. Orbach, and E. Simanek, Phys. Rev. 156, 383 (1967).

PHYSICAL REVIEW B VOLUME 3, NUMBER 10 15 MAY 1971

Excitation and Temperature Dependence of Band-Edge Photoluminescence in Gallium Arsenide†

V. I. Osinsky * and N. N. Winogradoff
National Bureau of Standards, Washington, D. C. 20234

(Received 18 September 1970)

Photoluminescent spectra of n-type GaAs were studied as a function of the excitation intensity, temperature, and doping level. The spectra consisted of two major bands representing radiative band-to-band recombination and radiative transitions through impurity centers, respectively. The intensity of the peak of the former went through a minimum and a maximum as the temperature was increased from 175 to 500 °K. The temperature corresponding to the above maximum increased as the excitation intensity was decreased or the doping level increased. These results suggest that the temperature dependence of the peak intensity in band-to-band transitions is primarily due to the thermal distribution of the carriers over the available energy states. The peak intensity would therefore normally be expected to decrease monotonically with an increase in temperature, while the above maxima and minima represent perturbations imposed by the presence of temperature-dependent transitions through radiative or nonradiative impurity recombination centers.

INTRODUCTION

Although the power output from luminescent GaAs p-n junctions generally decreases monotonically with an increase in temperature,[1] it has been found that the emission from GaAs diodes containing a high degree of compensation[2] in the p-type side of the junction passed through a maximum at a temperature which moved toward higher values as the current through the diode was reduced.[3,4]

This effect was explained in terms of a recombination mechanism which was governed by the position of the quasi-Fermi level for electrons which moved relative to radiative and nonradiative impurity levels in the forbidden gap, the former being attributed to donor states introduced by the compensating tellurium. However, the steep impurity gradients in the depletion region made it impossible to obtain unequivocal correlation of the above effects with the characteristics of the material in the emitting region, and there was always the possibility that the observed effects could be due to an injection[5] rather than to a recombination process.

In this work, direct correlation of these effects with the characteristics of the material and the re-